Supporting Information

General Strategy for Fabricating Transparent TiO_2 Nanotube Arrays for Dye-Sensitized Photoelectrodes: Illumination Geometry and Transport Properties

Jin Young Kim,[†] Jun Hong Noh,[‡] Kai Zhu,[†] Adam F. Halverson,[†] Nathan R. Neale,[†] Sangbaek Park,[‡] Kug Sun Hong,[‡] and Arthur J. Frank[†,*]

[†]*National Renewable Energy Laboratory, Golden, Colorado 80401-3393*
[‡]*Department of Materials Science and Engineering, Seoul National University, Seoul 151-744, Korea*

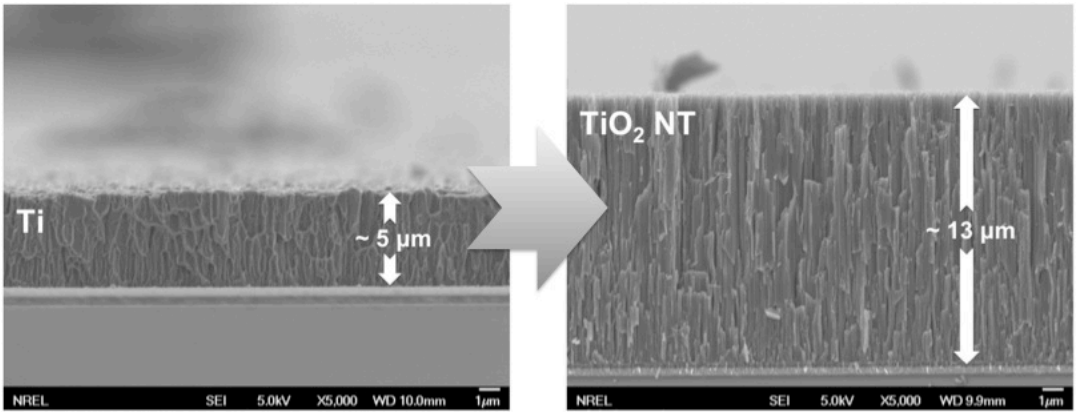

Figure S1. SEM images of a 5 μm-thick titanium film (left) used in preparing the 13 μm-thick titanium oxide NT film (right); the Ti film was deposited on an NTO/TCO substrate.

Figure S1 diplays the cross-sectional SEM images of a 5 μm-thick Ti film (left) and a 13 μm-thick titanium oxide NT film (right). The Ti film was deposited on an NTO/TCO substrate. The 13 μm-thick NT film prepared under the same electrochemical condition used for preparing the 6.4 μm-thick NT film described in the Method section in the main text. As in the case of the 6.4 μm-thick NT film, the 13 μm-thick NT film is 2.6 times thicker than Ti film from which it was prepared. This result is consistent with the discussion relating to Figure 1. The key point is that thicker NT films can be prepared on a transparent conducting substrate simply by depositing thicker Ti films on the NTO layer as described in this study.

*Address correspondence to Arthur.Frank@nrel.gov.

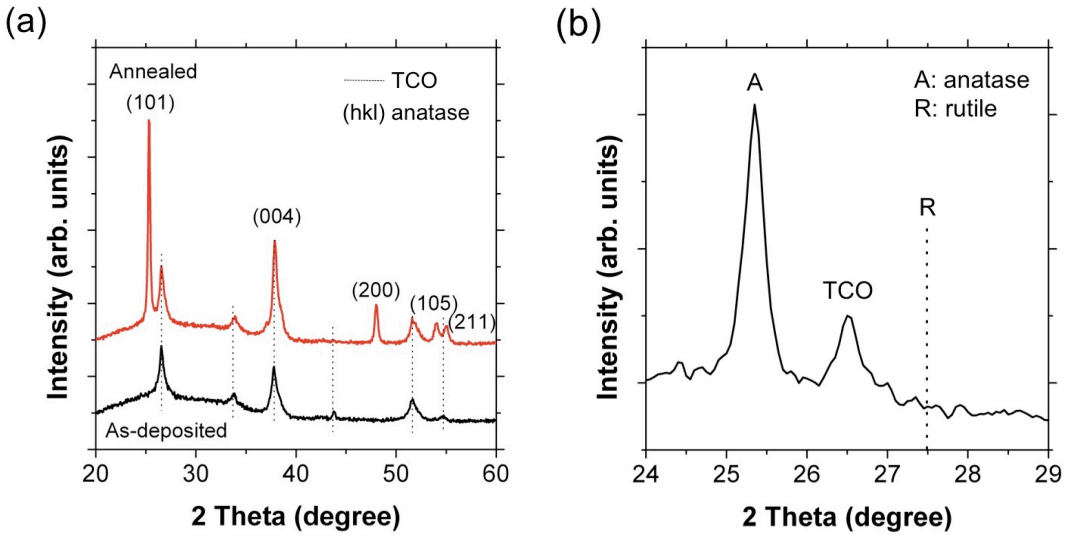

Figure S2. XRD patterns of a 6.4 μm thick titanium oxide NT film (a) before and after it was annealed at 400 ^{o}C and (b) after it was annealed at 590 ^{o}C.

Figure S2a shows the XRD patterns of an as-prepared and annealed transparent NT film grown on the NTO/TCO substrate. Only the diffraction patterns from the TCO substrate are observed for the as-deposited film, confirming that the Ti layer is completely converted to the amorphous TiO_x phase. Annealing the as-prepared NT film at 400 ^{o}C transforms it to the pure anatase TiO_2 phase; there is no trace of the rutile in the XRD patterns. Even at annealing temperatures at high as 590 ^{o}C (Figure S2b), there is no evidence for the formation of rutile, confirming the absence of Ti metal.[1]

Supporting Information

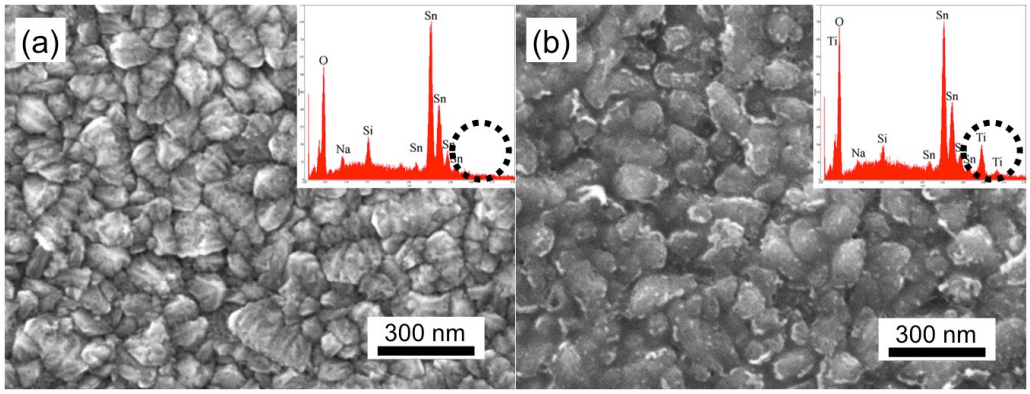

Figure S3. SEM images of (a) TCO and (b) NTO/TCO substrates after prolonged anodization of titanium layers. Insets in (a) and (b) show the corresponding EDS spectra.

Figure S3 shows the effect of prolonged anodization of Ti layers on TCO and NTO/TCO substrates. The EDS (inset) in Figure S3a indicates that after anodization of the Ti film on the TCO substrate only the tin oxide (TCO) remains – there is no spectral signature for elemental Ti – suggesting that the anodization process resulted in the detachment of the titanium oxide film from the TCO substrate. Therefore, the SEM image (Figure S3a) shows only the bare TCO surface. Figure S3b shows the surface of the NTO/TCO substrate after the NT film was intentionally removed from it following prolonged anodization. The EDS spectrum (inset in Figure S3a) shows the spectral signature for Ti along with tin oxide, confirming the presence of both the NTO layer and TCO substrate. These results concur with the conclusions drawn from the analyses of Figure 2 that the NTO layer prevents the direct exposure of the TCO substrate to the electrolyte along with the ensuing gas evolution and detachment of the NT film owing to the oxidation of the electrolyte and the TCO substrate.

Supporting Information

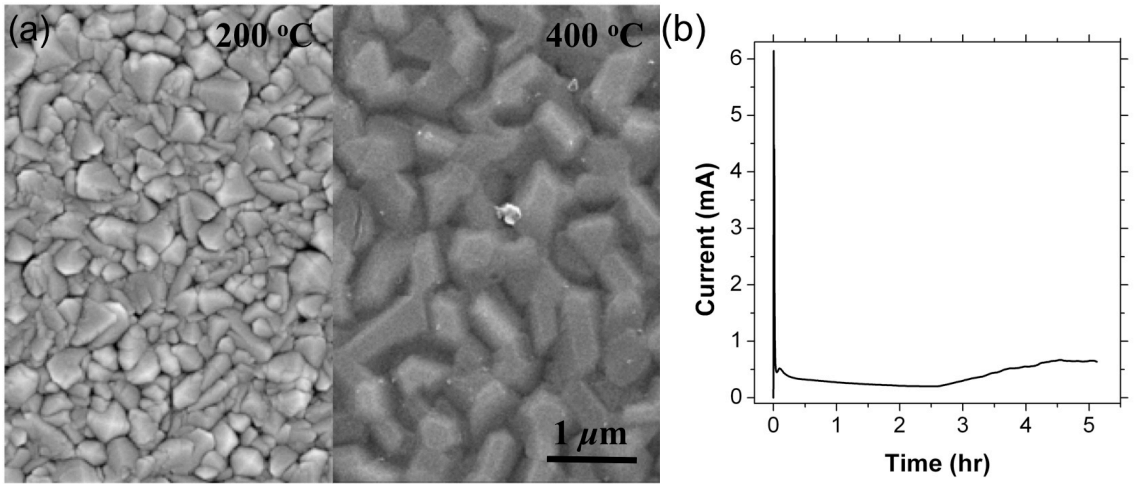

Figure S4. (a) SEM images of the surface morphology of Ti films deposited at 200 °C (left) and 400 °C (right). (b) Anodization current profile of the Ti film with the NTO layer deposited by PLD.

Figure S4a compares the surface morphology of a Ti layer deposited on a PLD-deposited NTO layer at 200 °C (left) and on a sputter-deposited NTO layer at 400 °C (right), the same deposition temperature used for the Ti film in Figure 2. The Ti film deposited at 200 °C has a smaller grain size and smoother surface than the 400 °C counterpart. Figure S4b shows the anodization current profile of a Ti layer deposited on the lower resistive PLD-deposited NTO layer at 200 °C. The Ti layer was anodized under similar conditions used in connection with Figure 2. Figure S4b shows that after the initial sharp rise and fall at the beginning of the anodization process, the current partially recovers and then gradually declines. The magnitude of this current drop and subsequent recovery in Figure S4b is much smaller than the one in Figure 2, an observation that is ascribed to the smoother surface[2] of the 200 °C-deposited Ti film compared with the surface of the 400 °C-deposited Ti film. After about 2.5 h, the NT film became transparent, signifying that the anodization was complete (discussions associated with Figure 2). Further anodization of the sample led to an increase in current along with gas evolution. Rinsing the resulting sample in water resulted in the detachment of the NT film. In contrast, for NT arrays grown on the higher resistive sputtered NTO layer, there was no sign of gas evolution or detachment of the NT films, even after they were thoroughly washed following prolong anodization. These results are consistent with the discussion relating to Figure 2.

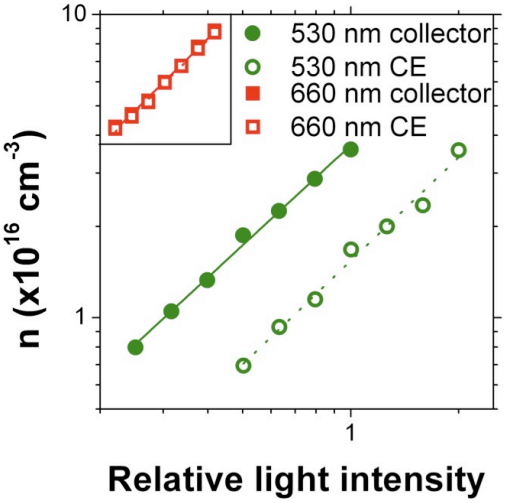

Figure S5. Photoelectron density of the 6.4 μm-thick TiO_2 NT-based DSSC as a function of the relative intensity of the 530 and 660 nm light pulses for collector-side and counter-electrode-side illumination; the inset show a log-log plot of the same data for 660 nm light.

Figure S5 shows the dependence of the photoelectron density of a transparent TiO_2 NT-based DSSC on the relative intensity of the 530 and 660 nm light pulses. The photoelectron densities display similar power-law dependencies on the light intensity, independent of the illumination geometry and wavelength of light. With 530 nm light, the counter-electrode side illuminated cell exhibits a 59% lower photoelectron density than the collector-side counterpart. The lower electron density is attributed to losses associated with the absorption of light by the electrolyte and recombination. An examination of the optical transmittance data in Figure 4a for the electrolyte-filled sandwiched TCO cell suggest that $\leq$ 41% of the light is absorbed by the electrolyte at 530 nm. Therefore, it follows that most of the photoelectron loss for the counter-electrode side illumination is due to light absorption by the redox electrolyte. The remaining portion of the difference in the photoelectron density ($\geq$ 18%) is ascribed to recombination. The photoelectron density of a DSSC illuminated with 660 nm light is the same for the two illumination geometries, which is consistent with the similar electrolyte light absorption and charge-collection properties. These results are in accord with the dependence of the IPCE spectra on the illumination geometry and wavelength of incident light in Figure 4a.

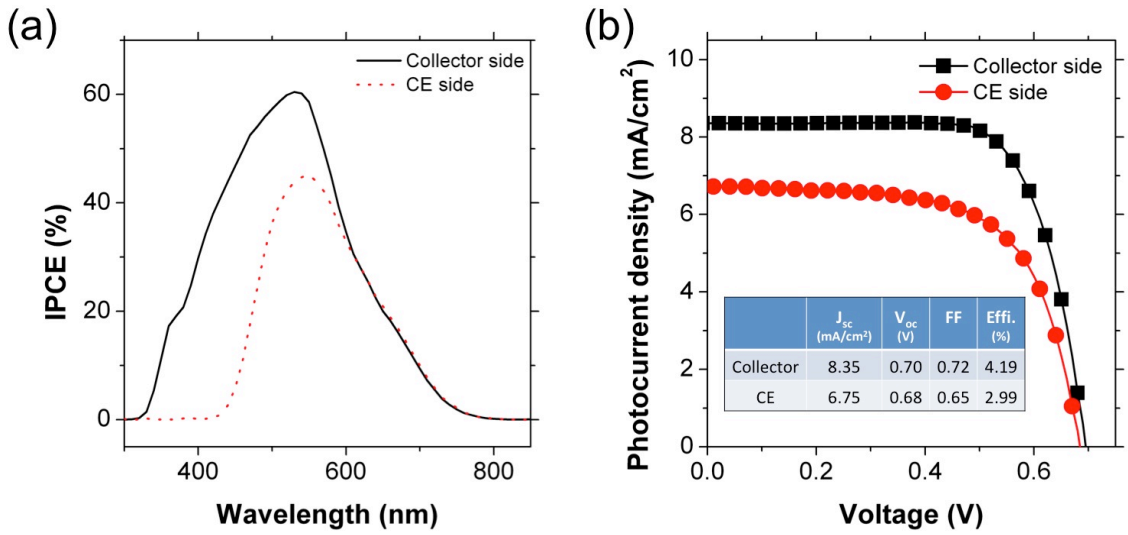

Figure S6. (a) IPCE spectra and (b) *J-V* charactertistics of TiO_2 NT-based DSSC containing a 13 μm-thick film (photoactive area ~0.12 cm^2). The cell was illuminated with simulated AM 1.5 light in (a), (b) from the collector side and counter-electrode side. Inset in (b) summarizes the *J-V* characteristics.

Figure S6 shows the effect of illumination direction on the short-circuit IPCE spectra and the *J–V* characteristics of a transparent DSSC constructed with a 13 μm-thick TiO_2 NT film. Figure S6a shows that the IPCE spectra of the DSSC with the 13 μm-thick NT film obtained with white bias light at 1 sun illumination intensity display the same trends as observed for the DSSC with the 6.4 μm-thick NT film (Figure 4a). When the light is incident from the collector side, the maximum IPCE occurs at 520 nm, whereas when it is incident from the counter-electrode side the maximum IPCE of the DSSC is observed at a longer wavelength, about 545 nm. For collector-side illumination, electrons are collected at about 340 nm and longer wavelengths. In contrast, for counter-electrode side illumination, no electrons are collected at wavelengths below about 430 nm. The difference in the relative magnitude of the spectral response from collector and counter-electrode-side illumination for the thick film (13 μm; Figure S6a) and thin film (6.4 μm; Figure 4a) is due to the optical path length through the electrolyte and the presence of the bias light. For the thicker NT film, the optical path length through the bulk electrolyte is reduced by the difference in film thicknesses, which is about 6.6 μm. The DSSC with the 13 μm-thick NT film was sealed with two layers of Surlyn thermoplastic, each 20 μm thick. This implies that the incident light from the CE side passed through about 27 μm of bulk electrolyte before entering the NT film. For the DSSCs with a 6.4 μm-thick NT film, the light from the CE side passes through 33.6 μm of bulk electrolyte. The absorption coefficient of the iodide-based electrolyte at 500 nm, calculated from the transmittance spectrum (Figure 4a), is 9.7×10^{-3} μm^{-1}. Therefore, the

approximate light attenuation by the bulk electrolyte is 53% and 45% for 6.4 μm and 13 μm NT samples, respectively. Moreover, a comparison of Figure 4a and Figure S6a shows that the difference in relative magnitude of the IPCE spectra for both collector and counter-electrode-side illumination is smaller for the thicker film than for the thinner. One of the reasons for the much smaller difference in spectral response of the DSSC with the thicker film is because a bias light was used. In the absence of a bias light, the time constant associated with the modulation frequency of the IPCE instrument is shorter than the response time of the DSSC. Thus, in the absence of a bias light, the IPCE measurements underestimate the values of the IPCE because most of the photogenerated charges are not collected due to the low photoelectron density. The underestimation is especially pronounced for counter-electrode side illumination because the photoelectron density is even lower than that for collector-side illumination. For example, Figure S5 shows that the photoelectron density for counter-electrode side illumination with 530 nm light is 41% of that for collector-side illumination. Overall, one can conclude from Figure 4a and Figure S6a that the photoresponse of the DSSC is larger and spectrally broader for collector-side illumination than for the counter-electrode-side illumination. The integrated values of the IPCE with the solar spectrum for the transparent DSSC with the 13 μm-thick TiO_2 NT film yielded a short-circuit photocurrent density of 7.9 mA/cm^2 for collector-side illumination, which is in good agreement with the measured J_{sc} (8.3 mA/cm^2; Figure S6a). Similarly, the integrated J_{sc} (5.8 mA/cm^2) from the IPCE measurement for counter-electrode-side illumination is comparable to the measured J_{sc} value (6.8 mA/cm^2). Figure S6b and the table insert show that the *J-V* characteristics exhibit similar dependence on the illumination geometry as noted for the DSSC with the 6.4 μm-thick NT film (Figure 5; Table 1). Photocurrent densities of the DSSC were larger for collector-side illumination than for counter-electrode side illumination while the illumination geometry dependence of the open-circuit photovoltage (V_{oc}) and the fill factor (*FF*) was less. On an absolute scale, however, increasing the film thickness used in the DSSC by twofold, from 6.4 to 13 μm, doubles the photoconversion efficiency. The DSSC with the 13 μm-thick NT film displayed a conversion efficiency of 4.2% compared with the 2.1% efficiency observed for the DSSC with the 6.4 μm-thick NT film (Figure 5); the 4.2% efficiency was measured with a mask to block spurious light from entering the cell and contributing to the photocurrent density. The increased conversion efficiency for collector side illumination is mainly attributable to the larger photocurrent density resulting from the thicker sensitized film and, to a lesser extent, the higher fill factor resulting from the reduced series resistance associated with the shorter ion diffusion length through the electrolyte. The latter is a consequence the decreased distance between outermost surface of the NT film and the counter electrode in DSSCs with the thicker film.

REFERENCES

1. Zhu, K.; Neale, N. R.; Halverson, A. F.; Kim, J. Y.; Frank, A. J., Effects of Annealing Temperature on the Charge-Collection and Light-Harvesting Properties of TiO_2 Nanotube-Based Dye-Sensitized Solar Cells. *J. Phys. Chem. C* **2010**, *114*, 13433-13441.

2. Shin, Y.; Lee, S., Self-Organized Regular Arrays of Anodic TiO_2 Nanotubes. *Nano Lett.* **2008**, *8*, 3171-3173.